1968

Ultimate load tests on braced multi-story frames, June 1968 (69-10)

J. A. Yura

L. W. Lu

Plastic Design of Multi-Story Frames

ULTIMATE LOAD TESTS ON BRACED MULTI-STORY FRAMES

by

Joseph A. Yura

and

Le-Wu Lu

This work has been carried out as part of an investigation sponsored jointly by the Welding Research Council and the Department of the Navy with funds furnished by the following:

American Iron and Steel Institute

American Institute of Steel Construction

Naval Ship Engineering Center

Naval Facilities Engineering Command

Fritz Engineering Laboratory

Department of Civil Engineering

Lehigh University

Bethlehem, Pennsylvania

May 1968

Fritz Engineering Laboratory Report No. 273.60

ABSTRACT

Four tests were conducted on three-story, two-bay fully welded frames fabricated from ASTM A36 steel. The frames were full size and were proportioned by the plastic design methods. Gravity, "checkerboard" and lateral loads were applied to the frames up to failure. The frames were braced against sidesway by diagonal bracing.

The tests were conducted to study the behavior and strength of braced multi-story steel frames and to evaluate plastic design methods for predicting frame behavior at maximum load. Theory is compared with experimental behavior in both the elastic and inelastic range. The experimental ultimate load reached or exceeded the maximum load predicted by plastic theory with an average discrepancy of 4%. The tests indicate that plastic design methods can be applied to braced multi-story frames.

TABLE OF CONTENTS

1. INTRODUCTION

In a steel structure subjected primarily to bending forces simple plastic theory can generally be used to determine the maximum load. Extensive experimental work has been completed on the components of such structures, that is, beams, columns and connections.[8] In addition full-size frame tests have been used to study the interaction among the components and thus establish the plastic method of analysis and design experimentally. These studies have shown that plastic methods are more rational and time saving compared to elastic or allowable-stress design methods for framed structures. The 1963 AISC specification permits the use of plastic design for low building frames in which the axial force in the column is relatively small and for beams in multi-story buildings provided that the columns are designed by allowable-stress methods.[13]

The restriction of plastic design to bending members has been warranted only by the lack of knowledge concerning the instability of members subjected to significant bending and axial forces (beam-columns) and the secondary moments and forces due to deformations. In recent years, however, Ojalvo[12] has solved the beam-column problem in that the load-deformation characteristics of a member can be predicted to maximum load and even after unloading. This solution was extended to an assemblage of members by Levi[10] and subsequent tests confirmed the approach.[9] These stability studies resulted in the formulation of a plastic design method for multi-story frames.[4] The design method depends on the

manner in which the frame resists lateral loads, that is, whether braced or unbraced. A braced frame relies on a vertical bracing system (such as diagonal bracing) or adjacent frames (through diaphragm action of the floor system) to resist lateral loads and sway. In an unbraced frame the bending stiffness of the beams and columns are depended upon to resist sway or drift.

In general terms the plastic design method for a braced multi-story frame consists first of choosing a beam section on the basis of the formation of a beam mechanism and then designing a column that can resist the beam moments at maximum load. This design approach is quite simple mainly because only beam mechanisms can form. In a braced frame the formation of sway-type plastic mechanisms is prevented by the bracing.[1]

A test program was initiated to study the behavior of braced multi-story steel frames loaded to failure and to evaluate plastic design methods for predicting frame behavior to maximum load. The results of this program which pertain to the overall behavior of the test frames themselves are presented herein. The interaction of the bracing and the frame in response to lateral loads is considered in another report.[15]

2. TEST PROGRAM

Maximum load tests were conducted on four braced frames. In all tests the frames had the same geometry and member sizes; only the loading condition varied for each test. The specimens were three-story, two-bay structures with columns 15 ft. center-to-center and with a total height of 30 ft. as shown in Fig. 1.

2.1 Test Frames

The test frames were proportioned by the plastic design method using load factors of 1.70 for gravity load and 1.30 for combined gravity and lateral loads.[4,11] Theoretically speaking, all structural components in the frames designed by this method would reach their maximum capacity at the same load. This was an idealization, however, since the actual selection of member sizes was based on available sections not minimum required sections. Nevertheless, based on the handbook section properties and a uniform yield stress of 36 ksi for all members, the design shown in Fig. 1 was balanced (within 1%). The diagonal bracing was designed to carry all the applied lateral load and minimize the second-order effects.[4,11] Continuous welded construction, Type 1 according to the AISC Specification,[13] was used on all the test specimens which were fabricated from steel conforming to ASTM-A36 Specification.[5]

The exterior columns were 6W20, the interior column 6W25 and all the beams 12B16.5. The strong axis slenderness ratio, L/r_x, of the columns was approximately 45, where L is the distance between two adjacent floors and r_x

the strong axis radius of gyration. The columns were continuous from the base to the top story, and the two beams at a story were cut from a single length of steel so that beam properties at a given story were as similar as possible. Two vertical loads were applied at 40.5 in. from the center line of each beam to simulate uniform loading. The top flange (compression) of each beam was braced laterally at 27 in. intervals ($35\ r_y$) between the two load points.[13] The bottom flange was unbraced throughout its entire length.

Each diagonal brace consisted of two 1-inch diameter rods. The design of bracing is discussed in Ref. 15. The diagonal bracing was prestressed by means of a turnbuckle before the testing operation to offset slackening in the bracing due to column shortening under axial load. The prestressing operation also permitted the measurement of the forces in the diagonal bracing.

Details of the rigid beam-to-column connections and the base condition assumed in the design and analysis are shown in Fig. 1. The connections were proportioned using standard plastic design procedures.[6] The interior connection did not require stiffeners. To approximate a fixed base condition, the columns were welded to a $2\frac{1}{2}$ in. base plate, which was prestressed to the foundation by two 3-inch diameter anchor bolts.

Each frame was shop fabricated in two large units, a one-bay, three-story frame and an exterior column with the adjacent beams attached. The units were fabricated under ordinary shop conditions with no unusual supervision or inspection. The two units of each frame were spliced

together in the laboratory.

2.2 Material and Section Properties

A36 steel was used for all the test frames. In order to minimize differences in materials, steel from only two heats was used. The columns, 6W29 and 6W25, were rolled from one heat and the 12B16.5 beams were rolled from a different heat. All members were cold-straightened by a continuous rotarizing process as standard shop procedure. Four types of tests and measurements were performed to determine the material and section properties: tension tests, cross-section measurements, beam tests, and residual stress measurements. A summary of these test results is given in the Appendix.

The measured section properties were within 5% of the handbook values, so handbook values of strong axis moment of inertia, I_x, were used for theoretical developments in this paper. The measured plastic moment, M_p, and axial yield load, P_y, showed a fairly wide range of values for each cross section, so the experimental values shown in Fig. 2 were used for individual members. Average experimental values were used for those members where no material property tests were conducted. On the average the actual M_p of the beam section was 11% larger than the value normally assumed in design, and the column sections were 18% larger. The measured P_y of the column sections was approximately 10% larger than the handbook values.

2.3 Loading Conditions

The loading conditions at ultimate for the four frame tests are given in Fig. 2 (the diagonal bracing of the frame is not shown for

clarity). The frame geometry was the same for all tests. Test 1 represented full factored dead and full factored live loading on all the beams. The loads on the top story were 0.75 of the lower level loads to prevent the formation of an isolated beam mechanism on the top story. This loading condition governed the plastic design of all members. A checkerboard loading arrangement was used in Test 2 which simulates full factored dead load on all the beams and full factored live load only on the beams of alternate bays and floors. This loading produces bending moments in the interior column. In Tests 3 and 4 the frames were subjected to lateral loading at each beam level in addition to the vertical loads shown for Tests 2 and 1 respectively. These lateral load tests were performed principally to study the effect of diagonal bracing in resisting lateral loads and the interaction of the diagonal bracing with the frame.

2.4 Test Setup

The test setup shown in Figs. 3 and 4 was similar in each bay on every floor. A single frame was tested in each setup. Vertical loads were applied to the test frame 40.5 in. from the center line of the beams. The two equal concentrated loads were applied to the beams through dynamometers (to measure the load) attached to the spreader beam which divided the single load supplied by the hydraulic loading system. Tension jacks had one end attached to the spreader beam and the other end connected to a gravity-load simulator.* The simulator was supported by

* The gravity-load simulator is a mechanism which permits the tension jack to remain vertical even after sidesway of the test frame, and it provides very little restraint against sway of the frame. It permits an approximation of gravity load using a hydraulic loading system. For a more detailed description, see Ref. 14.

the loading frame which was fixed to the foundation. Lateral loads were applied at each floor level by hydraulic jacks acting in tension. Movements of the test frame out of its plane was prevented by lateral bracing. Oil was distributed to the tension jacks by a control console which permitted a different load in each jack.

A more detailed description of the test setup and the equipment used for testing multi-story frames can be found elsewhere.[14,16]

2.5 Instrumentation

The loads applied to the test structures were measured by calibrated dynamometers. Pressure gages in the hydraulic lines provided another indication of the loads. Strain gages on the diagonal bracing were calibrated to indicate the forces in the bracing.

Strains were measured in each member of a test frame (nine in columns and six in beams) by electrical strain gages. Groups of four strain gages were placed at two locations in each beam. The moment and axial load at these two sections were calculated (with a sensitivity of 4 kip-in. and 0.9 kip respectively) from the strain readings and the known cross-section properties. Since the applied loads on the beams were also measured, the entire moment diagram for each beam was determined, independent of the other members at each load increment.

Strains and sidesway deflections at the center line and quarter points of each column were used to calculate the moment, shear and axial load. The sidesway deflection data permitted the second-order effects to be evaluated, resulting in more accurate shear and moment diagrams for the

columns.

Deflections of the structure were measured by transits and levels sighting on scales. Column deflections were measured at 30 in. intervals along their lengths, and the deflections of each beam were recorded at the ends, load points and center line. The rotations of the joints and bases in each frame were measured by electrical and mechanical gages.

3. FRAME BEHAVIOR

The analytical and actual behavior of the four braced frames are presented in this section. The loading conditions shown in Fig. 2 represent the final stage in the tests. The actual loading sequence was not always proportional for all the tests. The theoretical behavior is based on the actual loading sequence used in the tests and not on proportional loading.

3.1 Procedure for Developing Analytical Predictions

An elastic-plastic analysis was used to determine the maximum load by simple plastic theory, the order of formation of plastic hinges, and the load-deformation behavior of each test specimen. The center-line beam deflection was chosen as the deformation parameter for comparison with test results.

The analysis was based on the following assumptions:

1. The cross section was entirely elastic until M_p was reached and plastic behavior was assumed thereafter.
2. Plastic hinges could not form in the connections, only in the cross sections of the members at the faces of the connections.
3. Experimental values of M_p and P_y used in the analysis are given in Fig. 2. Handbook values for the section properties (moment of inertia, area, etc.) were used.

The load at which the first plastic hinge(s) formed was determined by an elastic analysis on the continuous rigid frame. At this load real

hinges were assumed at the plastic hinge locations and additional load was applied to this "altered" structure until the next plastic hinge formed according to an elastic analysis. The process continued, step-by-step, until enough plastic hinges formed to cause a mechanism.

3.2 Test Results

The structural behavior of each test frame is represented by a load-deformation curve, and the center-line deflection of the beams was chosen as the deformation criterion. The deflected shape of the frame at working load[2] ($P_{max}/1.7$) and at P_{max} is also given. The order in which plastic hinges formed is presented along with the moments at various locations in the critical members. An experimental plastic hinge was said to have formed in a particular member when the moment, based on strain data, reached the values shown in Fig. 2. In the case of columns the effect of axial load on the maximum bending capacity was considered.[3] Plastic hinges shown at the ends of a member are located at the faces of the connection, not at the center line of the member.

The loading condition for each test will be described using the general frame in Fig. 5 which also shows the system for locating each member and connection.

1. Test 1 - Full Gravity Load. The loading condition for this test represented full gravity loads on all the beams and no applied lateral load. Referring to the general loading condition shown in Fig. 5, $0.75\ P = P_1 = P_2$, $P = P_3 = P_4 = P_5 = P_6$, and $H = 0$. These proportions were maintained throughout the test.

The load-deflection curves for the beams at level 1 and the order

in which plastic hinges formed for the entire frame are shown in Fig. 6a. First yielding occurred in the beams at the interior connections of the lower two stories at P = 16.7 kips, and plastic hinges formed at these locations at P = 27.6 kips. Lateral buckling of the two lower-story beams was observed at P = 27.6 kips. At point c in Fig. 6a lateral movement at one of the bracing points in beam A-1-B was observed. A maximum load of 35.2 kips was reached in beam A-1-B and failure (defined as unloading) occurred when a local buckle formed in this beam at a braced point. The load-deformation curves show that the behavior of the two beams at the lower story was similar. The predicted maximum load was exceeded by 7%.

It was theorized that the local buckling might have been due to the extensive lateral buckling in the beams cause by movement of the braced points. Therefore, the structure was unloaded (dot-dash-line) and stiffeners welded at the sections where local buckling occurred. In addition the lateral bracing wassimproved to prevent movement of the braced point. The structure was re-loaded, and a maximum load of 35.2 kips was reached in beam C-1-B, the same maximum load as that for beam A-1-B. Plastic hinges formed at many locations throughout the structure as shown in Fig. 6a; beam mechanisms developed in both beams at level 1.

The deflected shapes of the beams for Test 1 are shown in Fig. 6b. The dashed curve represents deflections at $P_{max}/1.7$, and the deflected shape at maximum load (before unloading for repairs) is shown by the solid lines. The maximum deflections occur in the two beams at level 1 because of the formation of a mechanism.

The moments at four locations in the critical beam A-1-B are shown in Fig. 6c by the solid lines; the theoretical moments at the ends of the beam are shown by the dot-dash curves. There is good correlation between experimental and

theoretical behavior. M_p was first reached at the face of the interior column as predicted, but the moment continued to increase above M_p (up to 25% at maximum load) due to strain hardening. The bending capacity M_p was reached at three locations to constitute a theoretical beam mechanism. The redistribution of moments that took place within the beam after the first plastic hinge formed is shown by the increase in the slope of the curves for locations O and □ as P_{max} is approached. The moments shown at P = 0 were introduced by the initial prestressing of the diagonal bracing and the weight of the frame itself.

The moments in the exterior column at connection A1 are shown nondimensionalized by M_{pc} in Fig. 7 where M_{pc} is the theoretical bending capacity of the section considering the influence of axial load. At maximum load the column moments above and below the joint are at 0.95 and 0.88 of the theoretical bending capacity respectively.

2. Test 2 - Checkerboard Gravity Load. In this test loads representing factored dead load were placed on all beams and factored live load placed only on the beams of alternate bays and stories to provide a checkerboard loading condition. The test loading was applied in two main steps; first the factored dead load was applied, then the factored live load, in the following manner (referring to Fig. 5):

1. Dead Load $0 < P \leqslant 18.9$ kips

   $\frac{3}{4} P = P_1 = P_2$; $P = P_3 = P_4 = P_5 = P_6$; $H = 0$

2. Live Load $18.9 \text{ kips} < P \leqslant P_{max}$

   $\frac{3}{4} P = P_1 = P_2$; $P = P_4 = P_5$; $0 = P_3 = P_6$; $H = 0$

The load deflection curves for the two beams loaded with factored dead and live loads are given in Fig. 8a along with the order of plastic hinge formation. First yielding occurred in beams A-1-B and C-2-B at the face of the interior connections at P = 16.0 kips, and the first plastic hinge formed in beam A-1-B at the same location at P = 27.4 kips. At P = 32.8 kips first yielding was observed at the lower end of column 1-A-2 and lateral buckling started in beam A-1-B between the load points.

A maximum load of 35.1 kips was attained in A-1-B which was the same as the predicted maximum load. Plastic hinges formed at both ends of this beam while the maximum moment at load point reached 0.96 M_p. Unloading was caused by the formation of local buckles near midspan and at the ends. Beam C-2-B continued to carry additional load until a beam mechanism formed at P = 38.4 kips.

The deflection of the frame corresponding to working load ($P_{max}/1.7$) and maximum load in beam A-1-B are shown in Fig. 8b. The moment history at four locations in beam C-2-B is given in Fig. 8c; M_p was almost reached at all these locations. The moments in the beams at the faces of the interior and exterior connections exceeded M_p by 27% and 13% respectively.

3. Test 3 - Checkerboard Gravity Load and Wind Load. The loading arrangement at maximum load is shown in Fig. 2. There are many possible loading paths which would lead to this desired arrangement. It was decided to load the frame in the same manner that an actual building would be loaded while also considering the reduced factor of safety normally associated with combined gravity and wind loading.[13] The actual test loads were applied in four major phases, referring to Fig. 5:

1. Factored Dead Load $0 \leqslant P \leqslant 13.6$ kips

   $\frac{3}{4} P = P_1 = P_2$; $P = P_3 = P_4 = P_5 = P_6$; $H = 0$

2. Factored Live Load, $13.6 < P \leqslant 27.8$ kips

   $\frac{3}{4} P = P_1 = P_2$; $P = P_3 = P_6$; $0 = P_4 = P_5$; $H = 0$

3. Factored Wind Only, holding load from phases 1 and 2 above,

   $0 \leqslant H \leqslant 4.5$ kips

4. After the phases 1, 2 and 3 above were applied the loads had the approximate proportions shown in Fig. 2. These proportions were maintained until P_{max} (36.4 kips) was reached.

   $27.8 < P \leqslant 36.4$ kips

   $\frac{3}{4} P = P_1 = P_2$; $P = P_3 = P_6$; $\frac{1}{2} P = P_4 = P_5$; $\frac{1}{6} P = H$

The first three phases correspond to working load times a load factor of 1.3 for combined loading. Because full gravity load and not combined loading governed the frame design, the frame resisted the additional loads applied during phase 4.

The load-deflection curves for the two beams fully loaded are given in Fig. 9a. First yielding occurred in beam A-2-B at the interior connection at P = 17.1 kips during the second loading phase. A plastic hinge formed in beam C-1-B at the interior connection upon the completion of the second loading phase P = 27.8 kips. During the application of the wind alone (phase 3), no additional plastic hinges formed although there were some changes in the frame moments. Lateral buckling was observed in beams C-1-B and A-2-B at P = 32.1 kips and 35.6 kips respectively during the pro-

portional loading phase. The behavior of these two beams was similar up to a deflection of approximately 2 in. A mechanism formed in member A-2-B as predicted and the maximum load of 36.4 kips exceeded the theoretical value by 4%. The load did not drop off abruptly in Beam A-2-B as might be implied from the curve. The loads for both beams were placed in series on the same hydraulic line, and since most of the deformation occurred in Beam C-1-B, the apparent "sudden drop" in load on beam A-2-B resulted.

Actual unloading was due to local buckling in Beam C-1-B. At the maximum load plastic hinges had formed at both ends of Beam C-1-B while the moment at the load point was 806 kip-in. ($0.90\ M_p$). However, a maximum moment of 849 kip-in. ($0.98\ M_p$) was reached at the load point at a lower load (P = 35.4 kips), but lateral buckling caused a reduction in moment. The load increased from 35.4 kips to 36.4 kips even though the central portion of the beam was unloading, because of strain hardening at one of the ends. The moment in the beam at the face of the interior connection exceeded M_p by 21% at the maximum load.

The deflected shape of the frame at the maximum load is given in Fig. 9b along with the beam deflections at $P_{max}/1.7$. The column deforemations were so small at $P_{max}/1.7$ that they are omitted. The sidesway deflection at the top of column A was 0.48 in. Slightly larger sidesway deflections were recorded for column C because of the beam shortening resulting from the beam deflections. The diagonal bracing is not shown in Fig. 9b for clarity.

The moments in beam A-2-B are shown in Fig. 9c. M_p was reached at three locations to form a beam mechanism. The maximum beam moment at

the face of the interior beam-to-column connection exceeded M_p by 18% due to strain hardening.

4. Test 4 - Full Gravity Plus Wind Loads. The load proportions shown in Fig. 2, which were maintained throughout the test, represented full gravity loads on all the beams plus wind load. This particular test was used as a demonstration for a short course in plastic design methods, so the data recorded was greatly reduced compared to the previous three tests and the proportional loading arrangement was used for convenience.

The load-deflection response for the beams at level 1 is shown in Fig. 10a since mechanisms were expected to form in these members due to their lower available bending strength as indicated in Fig. 2. The order of plastic hinge formation is shown for all locations except level 3 where no data were recorded. First yielding and the first plastic hinge occurred in beam C-1-B at the face of the interior column connection. Failure (drop in load) resulted from local buckling in beam C-1-B. In addition to the plastic hinges in the beams throughout the structure, hinges formed in the exterior columns directly below the connections at level 1. The maximum load of 36.2 kips exceeded the theoretical failure load by 7%. The behavior of the two beams at level 1 was very similar.

The deflected shape of the frame at two load levels is shown in Fig. 10b. The maximum sidesway deflection was 0.42 in. at the top of column A. The moments for four location in beam A-1-B are shown in Fig. 10c. Strain hardening caused the moments at the ends of the beam to exceed the theoretical bending capacity (M_p) by 22%. The moments under the load points reached 0.96 M_p at maximum load, so that a theoretical mechanism almost formed. Beam C-1-B showed similar behavior, but the moment under one of the load point reached only 0.92 M_p.

4. DISCUSSION OF TEST RESULTS

In all four frame tests the maximum load predicted by simple plastic theory was reached or exceeded. The average excess for all the tests was 4%. In all cases, the theoretical maximum load was based on the formation of a beam mechanism using the actual material strength and not the minimum specified yield point normally assumed in design. The frame was intended to be a balanced design (all structural members chosen on the basis of their ultimate capacity), but the steel strength in the columns was somewhat higher than that assumed in the design. At maximum load in Test 1, the average end moments in the columns at connection A1 were within 8% of their theoretical capacity. Plastic hinges did form in the exterior columns in Tests 2 and 4 (see Figs. 8a and 10a), and a fairly balanced design was indicated by the extensive yielding in every frame at maximum load. The maximum axial loads in the columns reached $0.76\ P_y$ for the interior column and $0.40\ P_y$ for the exterior columns. The wind load had no significant effect on the capabilities of the braced frames to carry gravity load since the loads in Tests 3 and 4 exceeded the predicted maximum values based on simple plastic theory. The diagonal bracing was designed to carry all the lateral load. At early loading stages, the frames in Tests 3 and 4 did help to resist some of the lateral load; this is discussed more fully elsewhere.[15]

4.1 General Frame Behavior

Even though there were differences in loading and individual member strength among the four test specimens, the behavior of the four

frames was quite similar. First yielding and the first plastic hinge occurred in the beams at the interior beam-to-column connections as shown in Fig. 11 (this photo, as well as all subsequent photos, was taken after the completion of tests). The hinges were somewhat unsymmetrical because of the different joint details for the two beams as shown in Fig. 1. The field splice forced the plastic hinge to form in the beam at a greater distance from the column flange compared to the shop connection shown at the right in Fig. 11. The added stiffness of the field splice was one of the causes for the unsymmetrical formation of plastic hinges shown in Figs. 6a and 10a. (The wind load, sidesway-type moments of about 4% of M_p caused by the initial prestressing of the diagonal bracing, and rotation of some of the "fixed" bases were other factors.) The first plastic hinges formed at an average predicted load was 0.59 P_{max}. Actual hinges formed at a higher load than the predicted because redistribution of moments started with first yielding and the theoretical analysis assumed elastic behavior at a section until M_p was reached. The summary of tension tests given in the Appendix shows there was a significant difference between the yield points of material from the web and flanges of the 12B16.5. Based on average values, $M_p/M_y = 1.28$, whereas if the material strength is constant throughout the cross section $M_p/M_y = 1.18$. Consequently, in the test first yielding and the start of moment redistribution would be expected at 0.78 M_p.

Lateral buckling of the beams was first observed at 0.91 P_{max}, an average value for all frames except Test 1 where the lateral bracing system was faulty. Lateral buckling started at 0.78 P_{max} in Test 1. A typical beam is shown in Fig. 12 which includes only the portion of the beam load

points. The top (compression) flange is fairly well deformed laterally whereas the tension flange appears very straight. Only the compression flange was braced at the locations shown which were 27 in. apart (35 r_y). In general the lateral buckling started just after yield lines appeared between the load points. The load continued to increase despite the lateral buckling until large local buckles appeared near midspan and a slight local buckle occurred at one of the ends. A typical buckle between the load points is shown in Fig. 13 and slight local buckles can be seen in the bottom flange of the beams in Fig. 11.

The average maximum beam deflection at ultimate load was 2.4 in., and the deflection corresponding to working load was 0.5 in. This working load deflection results from both dead and live loads, so the live load deflection would be much less. Still, for this frame the total working load deflection was only 1/360 of the span. The sidesway deflection of Test 3 were larger than those of Test 4 because unsymmetrical gravity loads contributed to the sidesway for the former case.

The moments in the beams in the elastic range and at maximum load are shown in Fig. 14 for a frame with a symmetric unit gravity load. The experimental unit moments in the elastic range were determined by dividing the test moments by the actual load on the structure. The particular load level chosen to evaluate the experimental unit moments was the maximum load in the elastic range. Since the loading arrangements of all four tests included at least an initial application representing symmetric dead load, the solid lines on the left portion (elastic) are the average of all tests. The theoretical dashed lines were determined by computer analysis using handbook section properties and center-line distances for the lengths of the members. The

theory showed slightly higher maximum moments than actually recorded. Although it is not shown, an elastic analysis based on clear dimensions for lengths showed better correlation with test results. The unit diagram at maximum load were determined in the same way as the elastic values except only Tests 1 and 4 were used due to the similar load proportions (full gravity) at P_{max}. There is good correlation between test and theory. The redistribution of moments that takes place from the elastic range to ultimate load is obvious in this figure. At ultimate load the moment diagram for each beam tends to become symmetrical except at the top level where no attempt was made to reach the maximum load.

Although Fig. 14 shows good correlation between test and theory for the elastic range and maximum load, the moment-load relationship for a particular location in a frame could not generally be predicted for the entire load cycle. The comparison between test and theory in Fig. 6c for the end moments in one of the beams of Frame 1 does dhow good correlation, but a comparison of Figs. 6c and 10c shows that the experimental values vary substantially for the two tests while the theoretical prediction for Test 4 would be practically identical to Test 1. Test results given in Figs. 8c, 9c and 10c were not compared directly with theory for clarity. Similarily, the order of plastic hinge formation could not be predicted very well although the first hinge and the final beam mechanism were predictable. The difference between test and theory for the load-moment history and the order of plastic hinge formation resulted from plastic hinges and yielding not being confined to localized areas, significant and variable rotation of the fixed bases, and a difference in the flexibility of the connections due to different axial load at each level (the last effect will be discussed later).

4.2 Behavior of the Critical Beams

In all tests the frame strength was determined by failure (unloading) of a fully loaded beam after extensive yielding occurred throughout the structure. The average moment diagram at P_{max} for seven beams in which failure was expected and/or occurred is shown in Fig. 15 by the solid lines, and the range of data is given by the heavy dots. The summary includes results from all four frame tests. The moment diagram is based on recorded joint moments that satisfied joint equilibrium within 2% of the beam M_p, so the data is reliable within this percentage. The average beam moment at the interior face was 22% above M_p with a rather narrow range of 19-26%. At the face of the exterior column the beam moment ranged from 0.99 M_p to 1.22 M_p with an average of 1.09 M_p; the wide range was due mainly to the "fixed base" rotations, the different vertical load arrangements on each frame and the wind load. The average moment under the load point at C at P_{max} was 0.96 M_p.

Failure initiated in one of the beams at level 1 in all four tests. This was expected in Tests 1, 2 and 4 because of the relative beam strengths shown in Fig. 2. In Test 3, however, a beam mechanism was not predicted at level 1 since the beams at level 2 had a lower bending strength. The principal reason for this discrepancy was lateral buckling between the two load points which usually followed the formation of the bending yield lines at this same location. Yielding between the load points was always first expected at level 1 because of larger theoretical exterior joint rotations. However, the midspan yielding started earlier than predicted because of "fixed base" rotations, and increased rotations within the joint itself due to axial load.

After significant lateral buckling the midspan moments decreased, but the corresponding higher moments at the ends of a beam resulted in a net increase in applied load. The moments at points C and D in Fig. 15 refer to the condition at maximum load; in Tests 1, 2 and 3 higher moments were actually recorded at these positions at lower load levels. The bracing spacing was one contributing factor to lateral buckling and the subsequent midspan moment reduction. The 35 r_y rule[13] for bracing spacing which was used in the frame design assumes elastic sidespans, immediately adjacent to the yielded critical section. For yielded sidespans, a condition present in all the frame tests, the spacing should be reduced to 25 r_y (See Ref. 4). Secondly, the current theories summarized in Ref. 4 show bracing spacing and local buckling are functions of the strain hardening modulus E_{st}. The assumed value of E_{st} = 900 ksi used in the theories does not compare very favorably with the average E_{st} = 314 ksi for the 12B16.5 flange given in Table A1.

In spite of the larger bracing spacing and the low available strain hardening modulus, moment redistribution did take place, and the theoretical load was reached or exceeded.

4.3 General Observations

Some general observations concerning structural behavior which have not been presented elsewhere in this paper are given below:

1. Predicted maximum loads were attained even though there was no lateral bracing along the bottom flange of all beams.
2. There was better correlation between test and theory when the structural analysis was based on clear spans and heights rather than center line dimensions.
3. In Test 1, the frame responded in an elastic manner when unloading occurred even though the frame was highly yielded

and beam buckling had occurred.

4. The interior beam-to-column behaved satisfactorily. In the field splice portion shown in Fig. 1, the beam web was not welded directly to the column, yet moments exceeding 20% of the beam M_p were successfully resisted.

5. Plastic design procedures indicated that column stiffeneres were not required in the interior beam-to-column connection and no stiffeners were used in Test 1. However, lateral buckling of the beams distorted the column flanges as shown in Fig. 16. Without stiffeners, each column flange provided essentially a pinned support for lateral bending of the attached beams. In Tests 2, 3 and 4 the column flanges were stiffened by plates (shown dashed in Fig. 16) in line with the bottom beam flange to prevent this column flange distortion. The desired effect was achieved, and, in addition, lateral buckling of the beam in the vicinity of the interior connection was prevented by the greatly increased lateral stiffness of the column flanges. Theory indicates that an elastic lateral buckling load can be increased about four times when the minor axis end conditions are charges from "pinned" to "fixed". The column stiffeners in Tests 2, 3 and 4 were used only as a precaution. There is no evidence that the column distortion observed in Test 1 affected the strength of the frame, especially since the maximum load exceeded the theoretical ultimate load.

6. Because the actual order of plastic hinge formation is not readily predictable, design rules which permit larger bracing spacing at the plastic hinge that forms last should be approached with caution. If practical, bracing by plastic rules should be used in the vicinity of all plastic hinges.

5. SUMMARY AND CONCLUSIONS

Four tests were conducted on three-story, two-bay, full size rigid frames fabricated from A36 steel and proportioned by plastic design methods. The principal purpose of the tests was to evaluate plastic design methods for braced multi-story frames. Ths most important observations are summarized below:

1. All four tests reached or exceeded the predicted maximum load by plastic theory. The average discrepancy was about 4%.
2. The distribution of moments throughout the structure was altered by "fixed-base" rotations and generalized yielding (rather than the localized yielding confined to plastic hinge locations assumed in the design method), but P_{max} was not affected.
3. The order of plastic hinge formation varied from the theoretical sequence, but P_{max} was not altered.
4. The formation of plastic hinges in the columns did not prove to be detrimental and the behavior was readily predictable.
5. The lateral (wind) load had no significant effect on the capabilities of the braced frame to carry gravity load. (The diagonal bracing was designed to resist all the lateral load).

The tests indicates that plastic methods can be applied to the design of braced multi-story frames.

6. ACKNOWLEDGMENTS

The work reported herein was performed at the Fritz Engineering Laboratory, Department of Civil Engineering, Lehigh University. The results presented form part of a general investigation on "Plastic Design of Multi-Story Frames." Sponsorship for the program was provided by the American Iron and Steel Institute, the American Institute of Steel Construction, Naval Ship Engineering Center, Naval Facilities Engineering Command and the Welding Research Council. Technical guidance was provided by the Lehigh Project Subcommittee (T. R. Higgins, Chairman) of the Welding Research Council. George C. Driscoll, Jr. and Theodore V. Galambos directed the overall program.

The research which was conducted could not have been performed without the assistance of many of the writers' colleagues. Special contributions toward the test setup, testing and structural analysis were made by E. Yarimci and B. A. Bott. R. G. Slutter and K. R. Harpel helped with the practical aspects of the test setup.

7. FIGURES

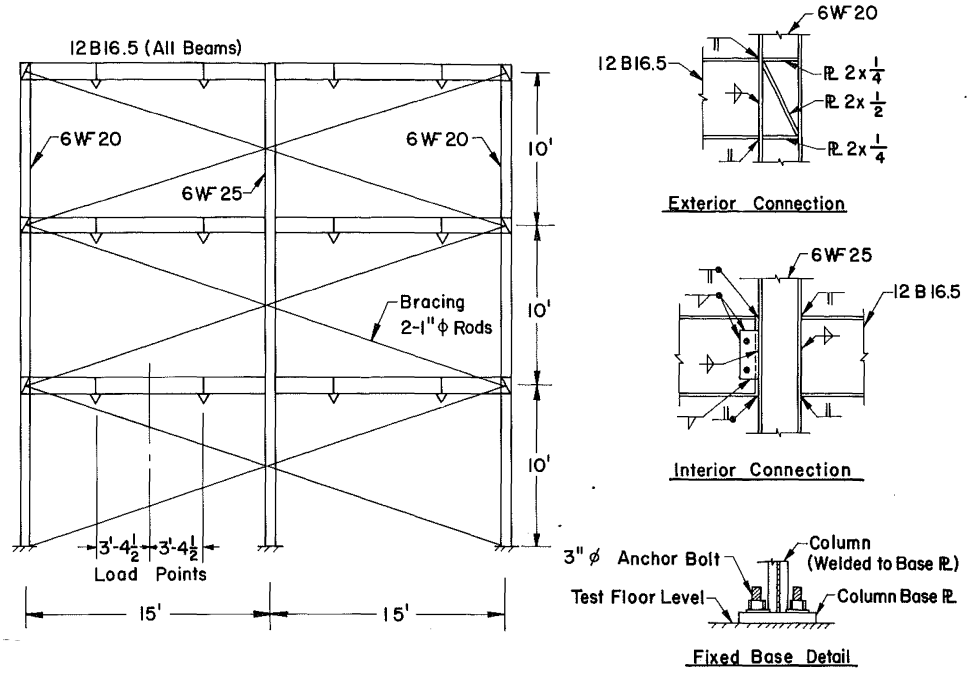

FIG. 1 TEST SPECIMENS

TEST NO.	1	2	3	4
LOADING CONDITION AT ULTIMATE LOAD	Full Gravity .75P .75P P P P P C B A	Checkerboard .75P .75P P .5P .5P P C B A	Checkerboard + Wind .75P .75P .167P .5P P .167P P .5P .167P C B A	Full Gravity + Wind .75P .75P .167P P P .167P P P .167P C B A
MEASURED MATERIAL PROPERTIES M_p kip-in. (P_y) kips	826* 822 773 635* 818 635* (243)* (292) (243)* *Average Value	826* 837 838 648 758 601 (243) (290) (234)	826* 837 870 620 800 649 (242) (299) (242)	826* 864 781 635* 744 641 (243)* (286) (252)

FIG. 2 TEST PROGRAM

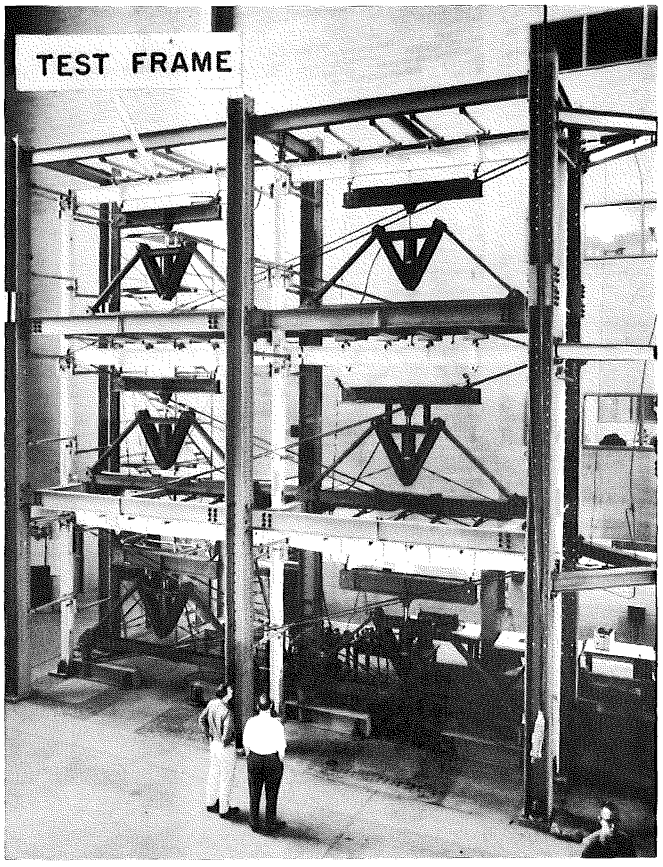

FIG. 3 OVERALL VIEW OF TEST SETUP

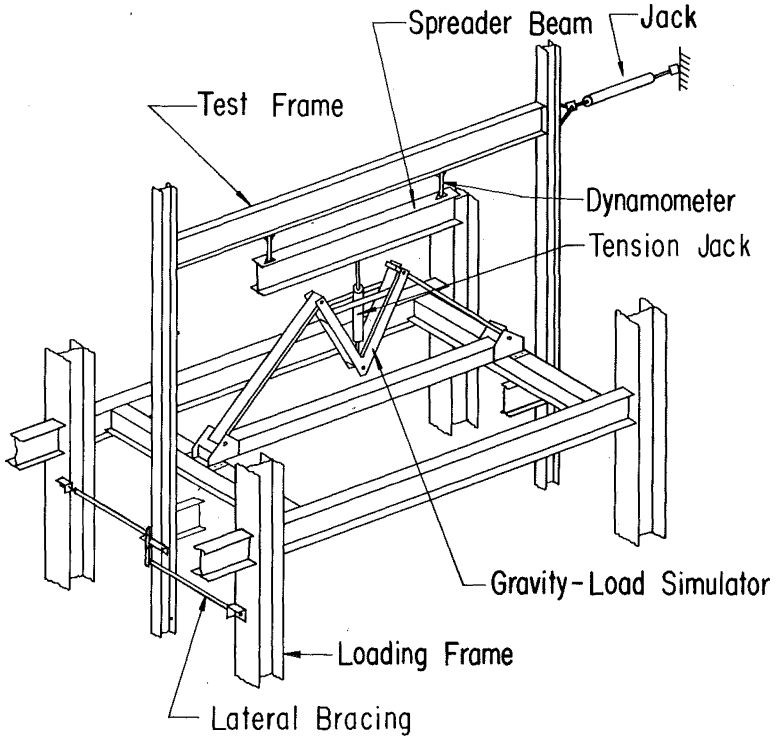

FIG. 4 TYPICAL BAY OF TEST SETUP

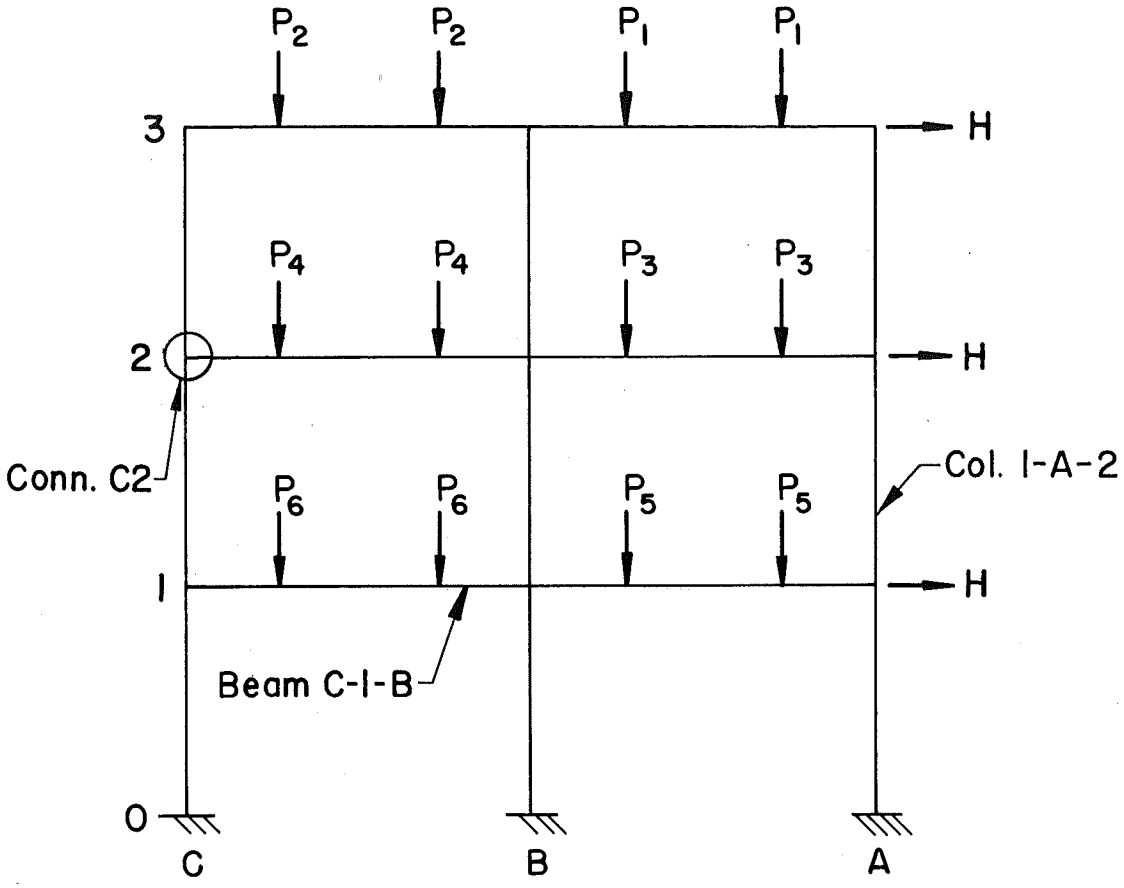

FIG. 5 GENERAL LOADING CONDITION AND IDENTIFICATION SYSTEM

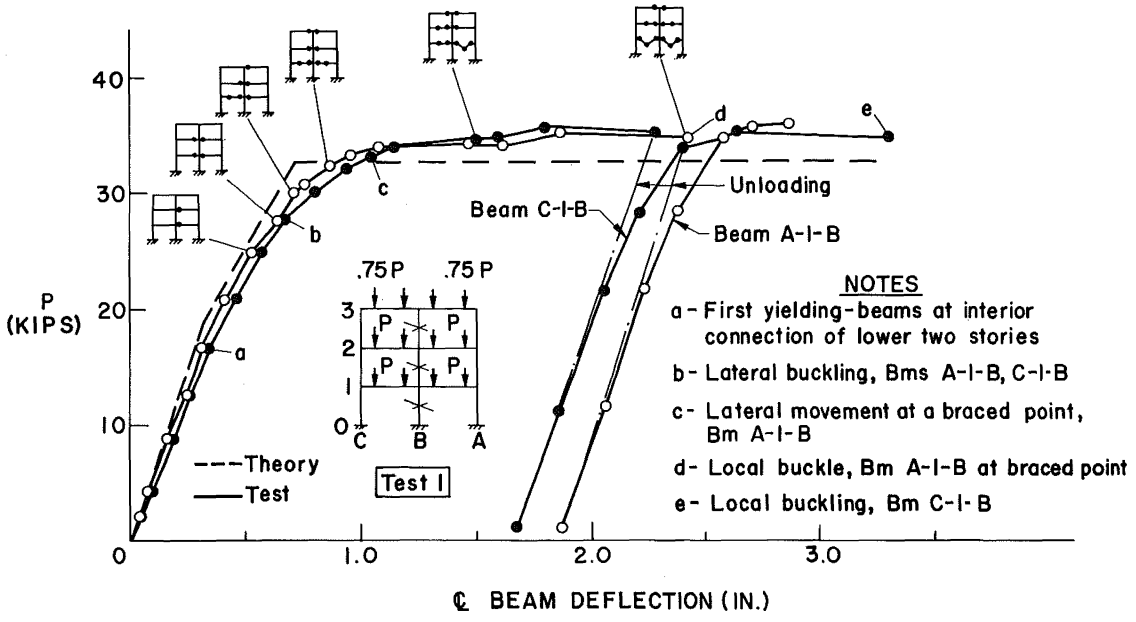

(a) Load-Deflection Relationships

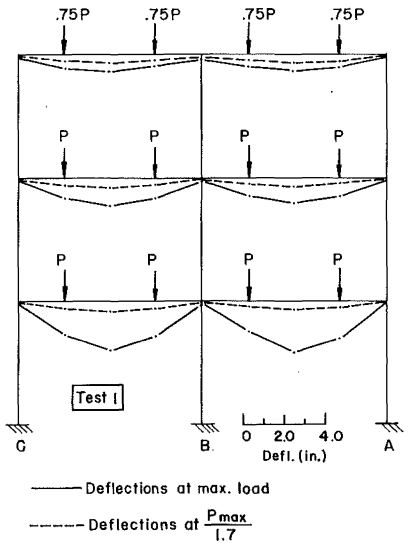

(b) Frame Deflections

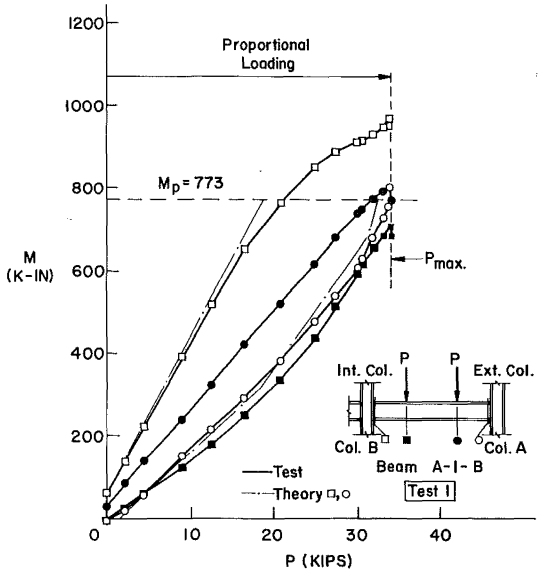

(c) Beam Moments

FIG. 6 RESULTS OF TEST 1

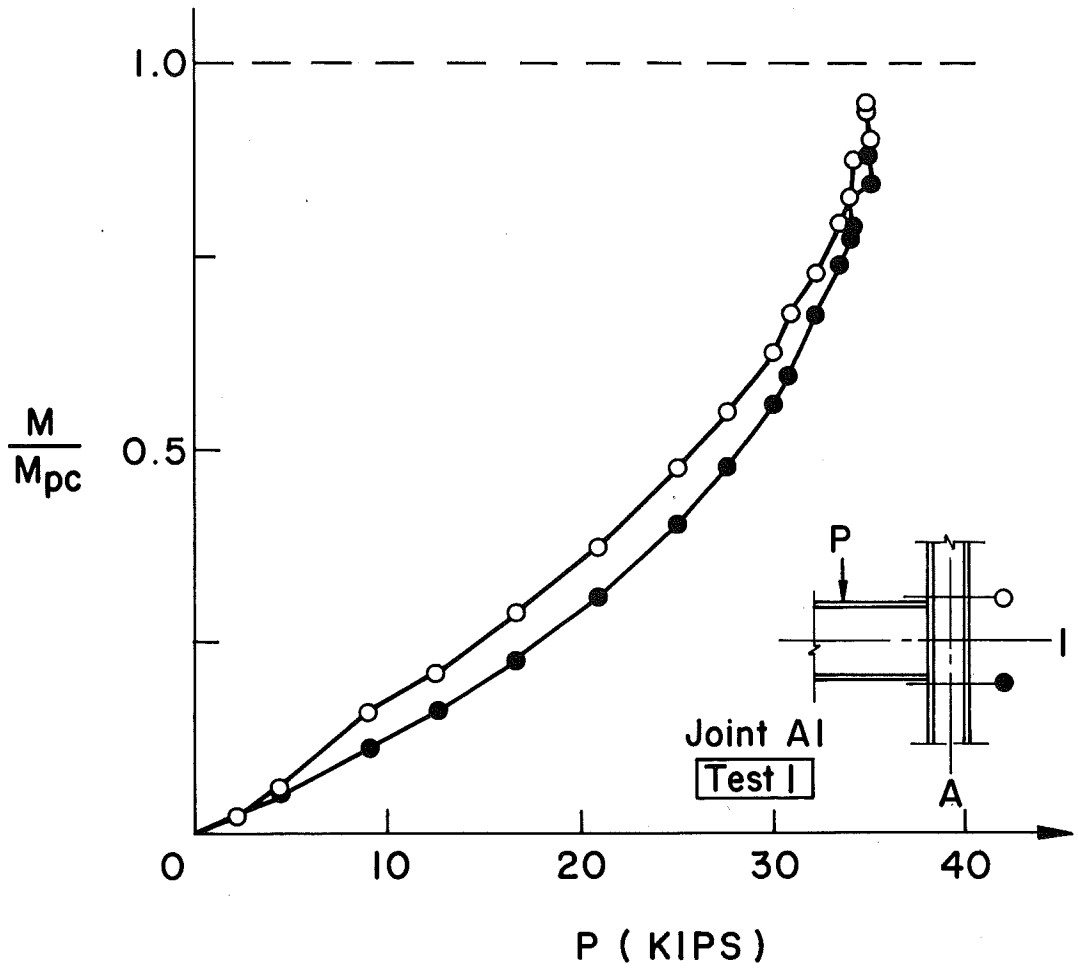

FIG. 7 COLUMN MOMENTS AT JOINT A1-TEST 1

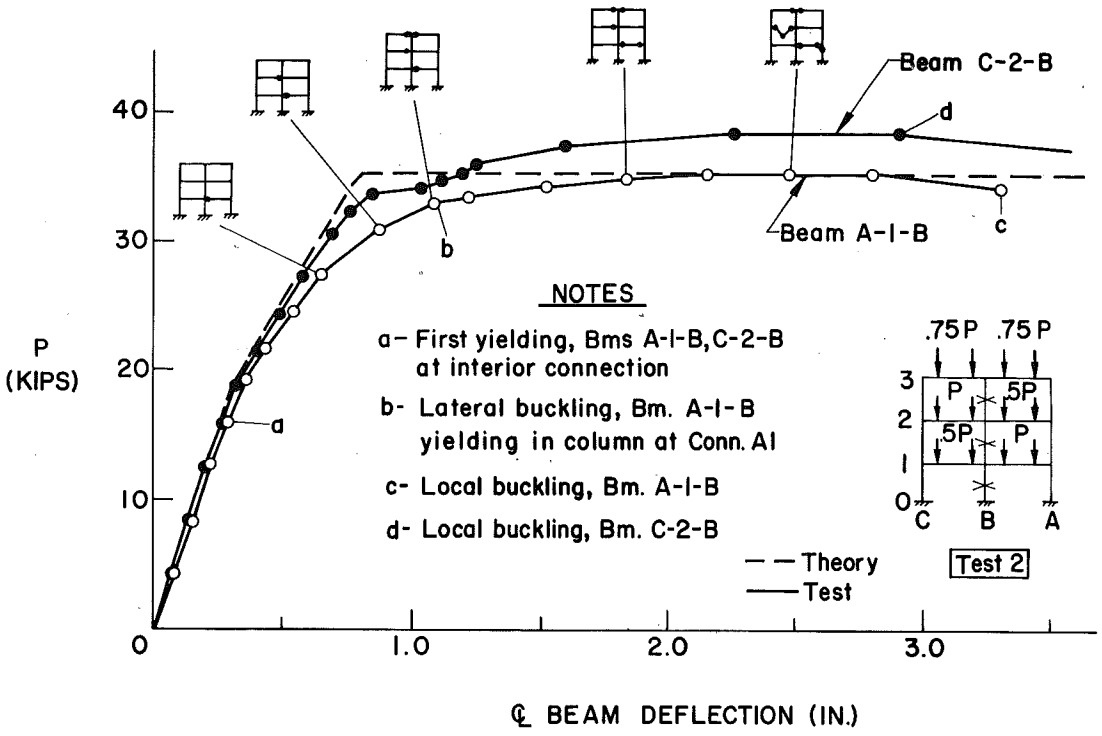

(a) Load-Deflection Relationships

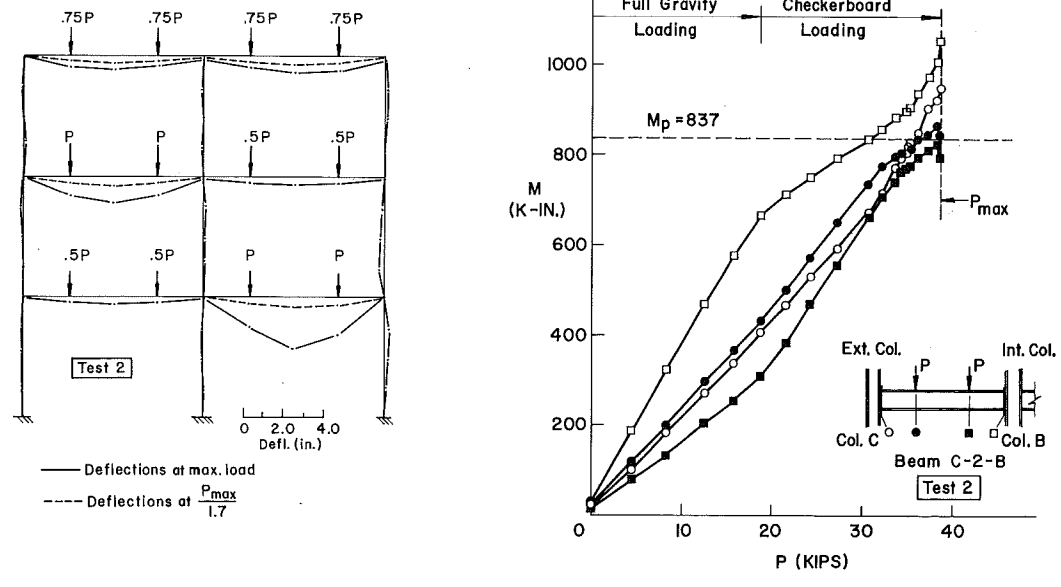

(b) Frame Deflections

(c) Beam Moments

FIG. 8 RESULTS OF TEST 2

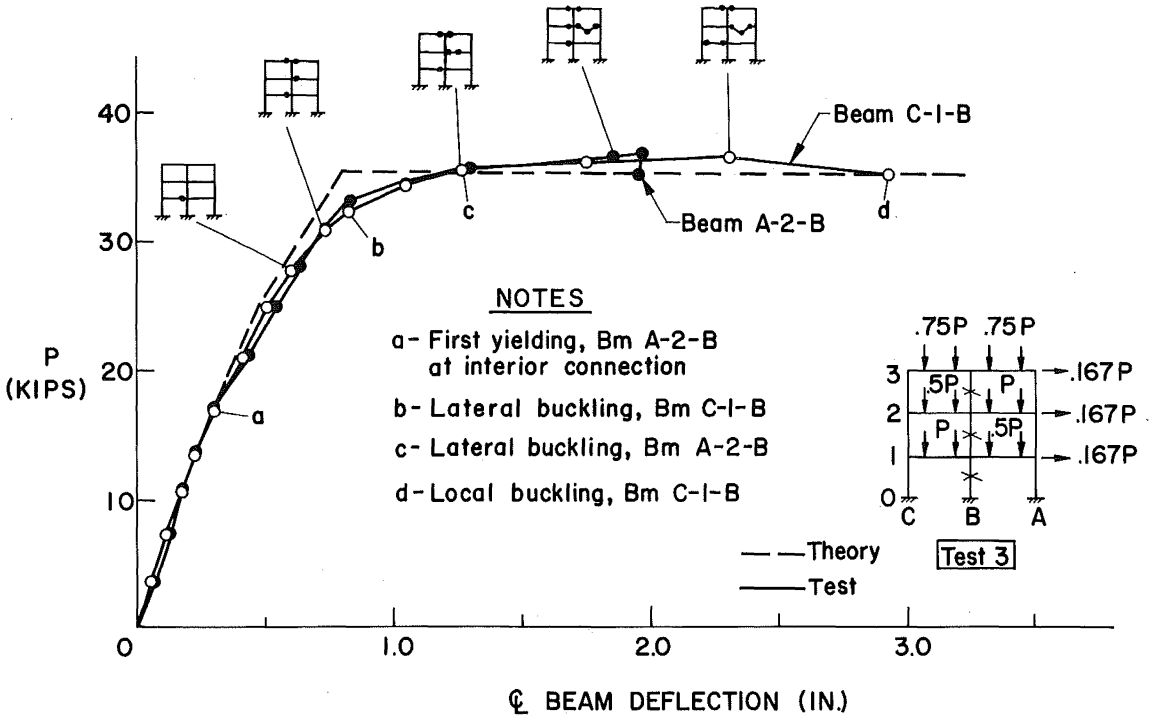

(a) Load-Deflection Relationships

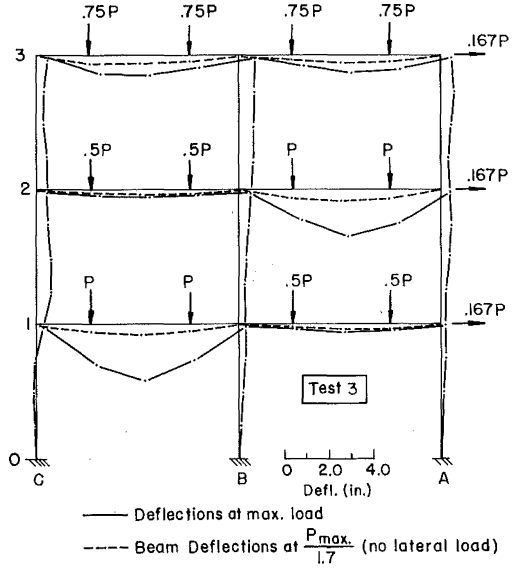

(b) Frame Deflections

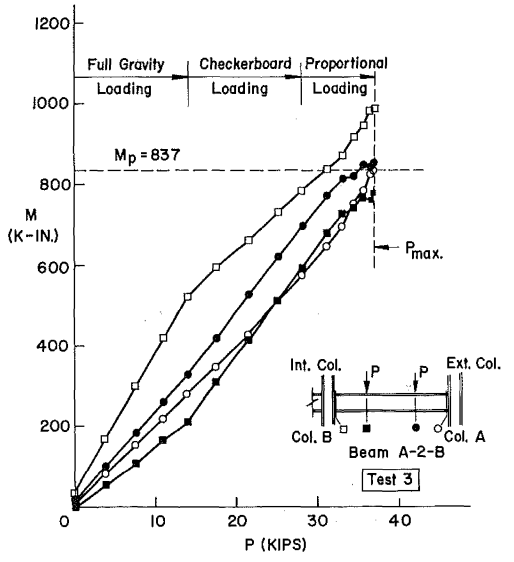

(c) Beam Moments

FIG. 9 RESULTS OF TEST 3

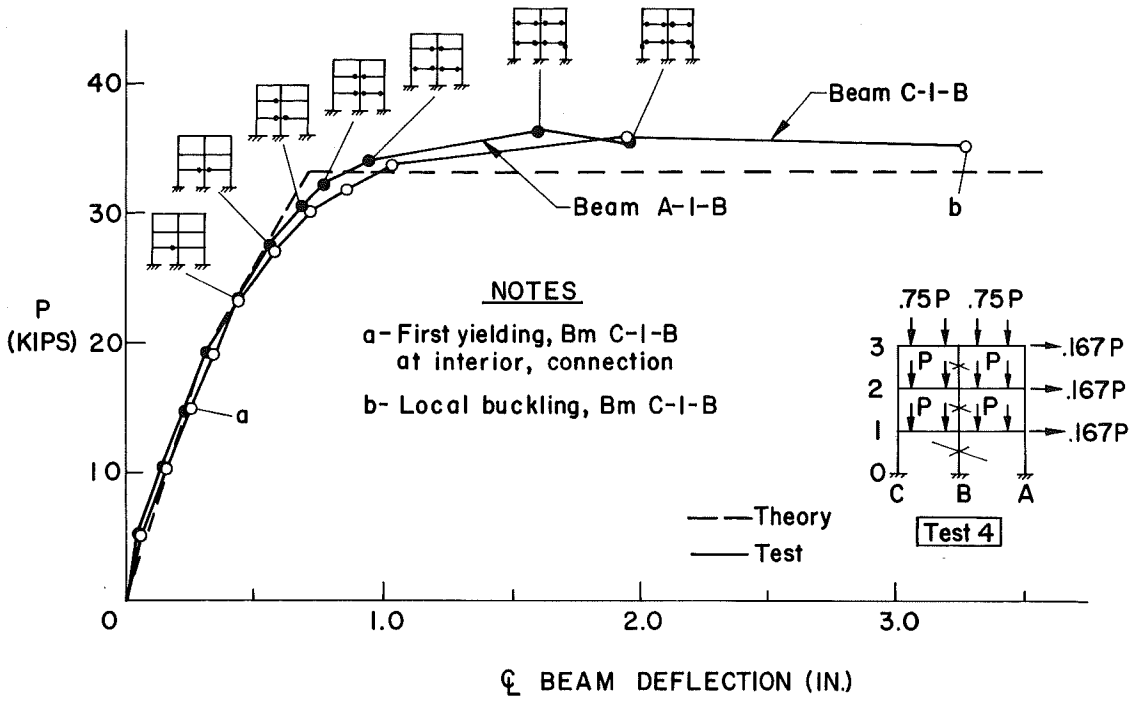

(a) Load-Deflection Relationships

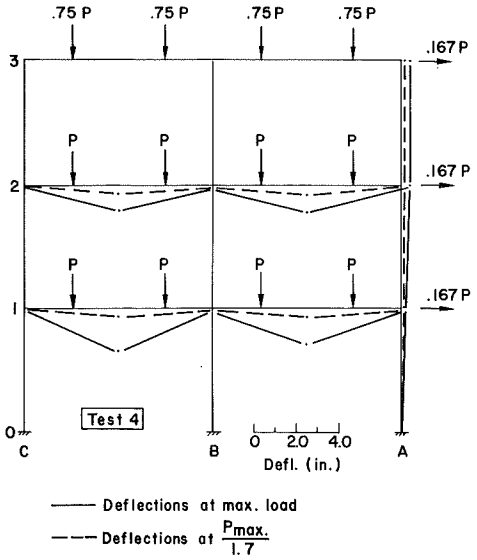

(b) Frame Deflections

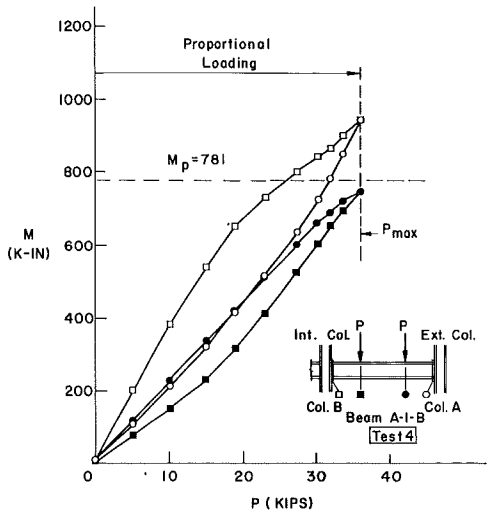

(c) Beam Moments

FIG. 10 RESULTS OF TEST 4

FIG. 11 INTERIOR CONNECTION WITH HINGES IN BOTH BEAMS

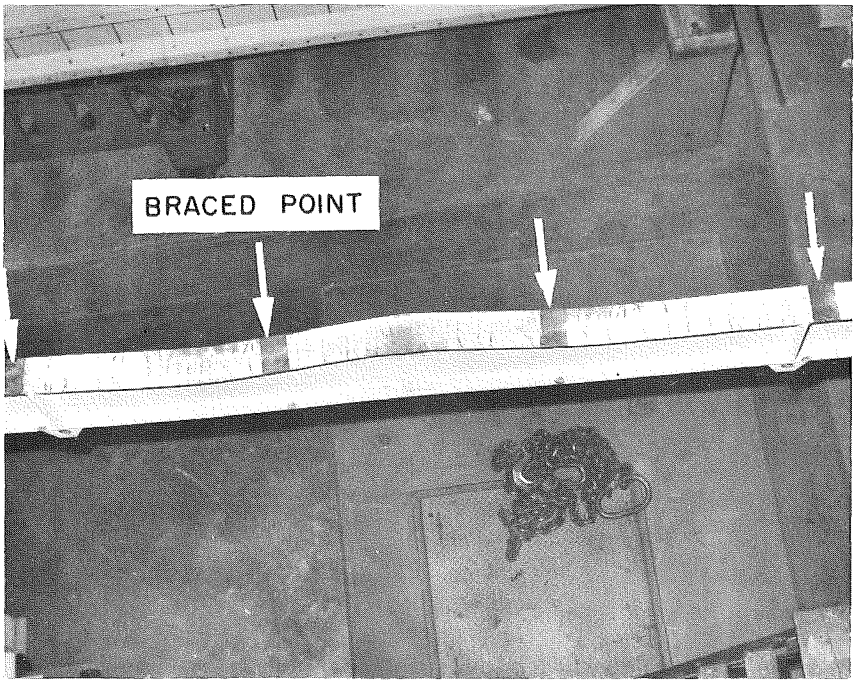

FIG. 12 LATERAL BUCKLING OF BEAM AT MAXIMUM LOAD

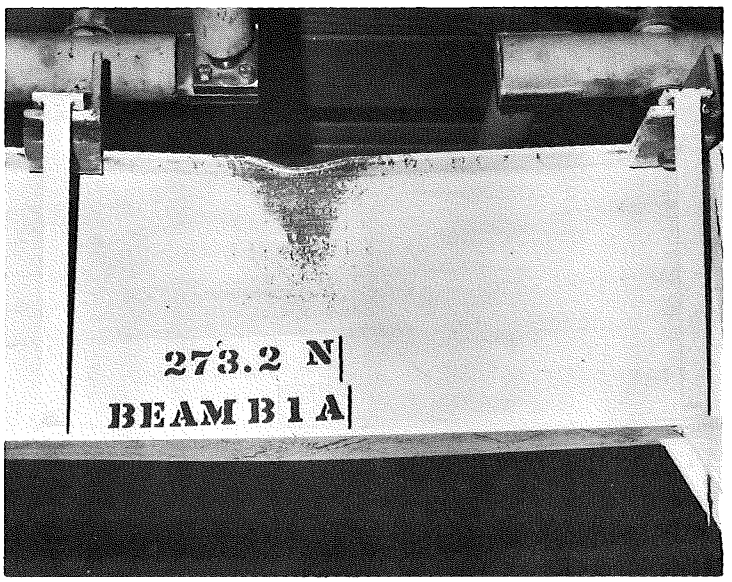

FIG. 13 LOCAL FLANGE BUCKLING IN BEAM

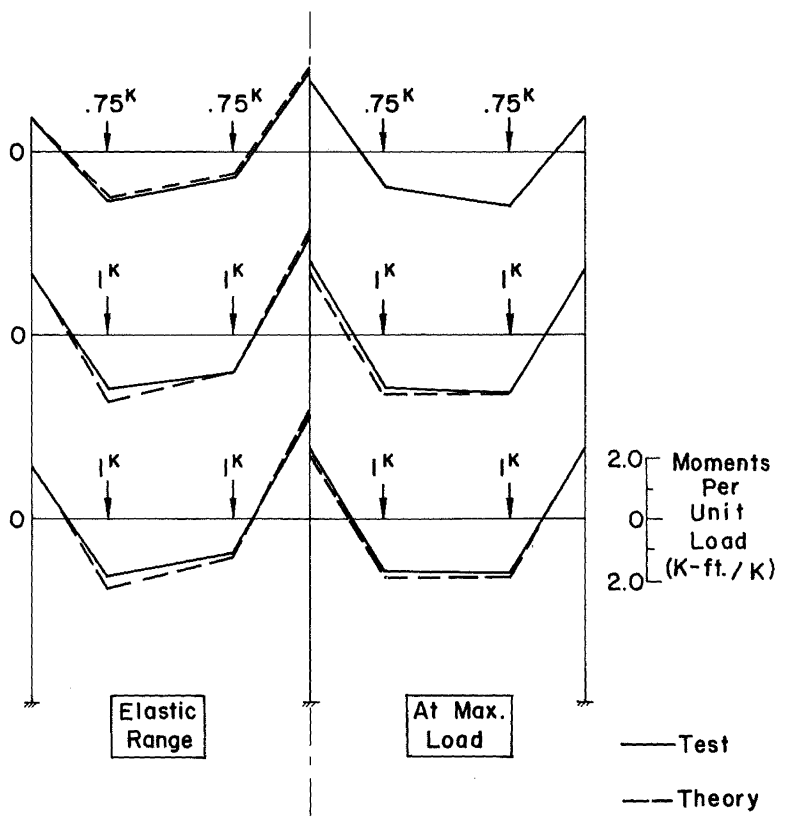

FIG. 14 UNIT-LOAD MOMENT DIAGRAMS

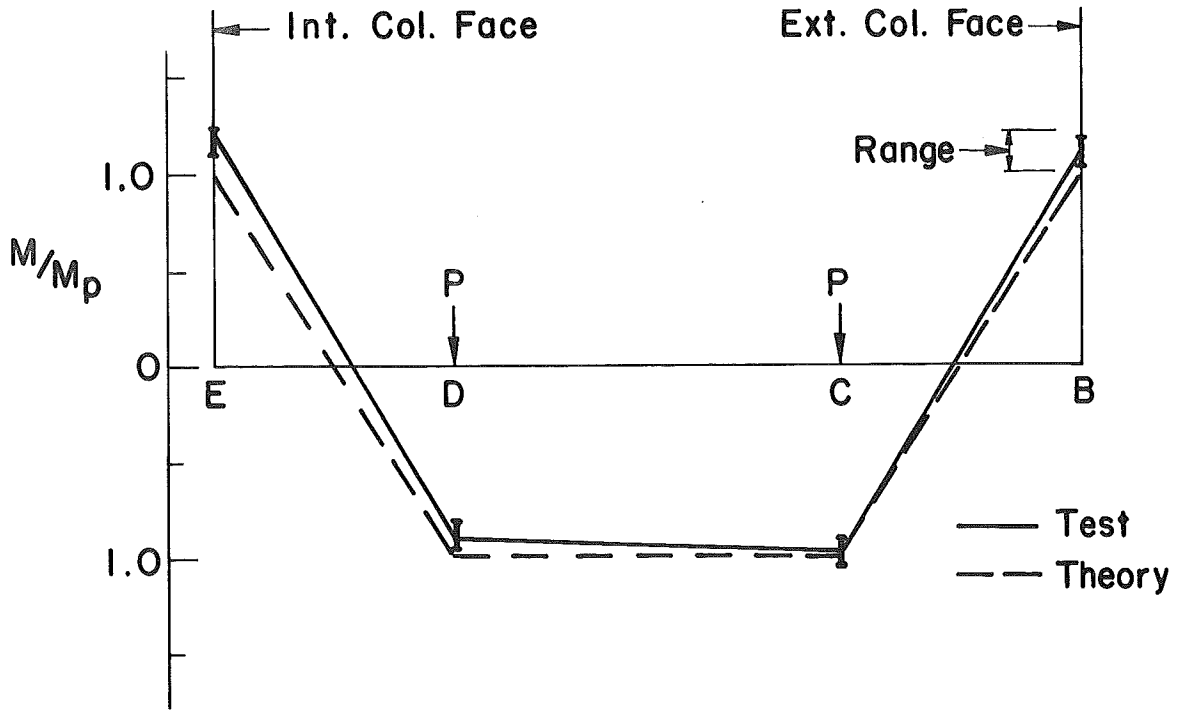

FIG. 15 AVERAGE BEAM MOMENT DIAGRAM AT P_{max}

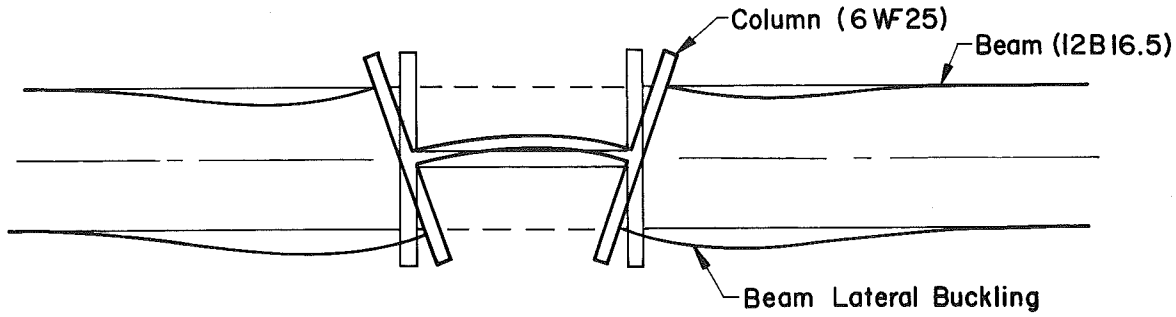

FIG. 16 COLUMN FLANGE DISTORTION

8. APPENDIX MATERIAL AND SECTION PROPERTIES - TEST RESULTS

1. Tension Tests. A summary of the tension tests conducted is given in Table A1. Flange and web data are shown separately since web specimens often have a higher yield stress than flange specimens.[2] The static yield stress, σ_y, ultimate stress, σ_u, percent elongation in 8 in., strain-hardening modulus E_{st}, and ratio of strain at strain-hardening to yield strain, ϵ_{st}/ϵ_y, are given. It was standard procedure to cut three tension specimens at any section, one from an edge of each flange and one at the center line of web. This enabled the bending capacity of a cross section to be calculated when the section properties were measured.

The statical yield stress of 20 flange specimens from the 12B16.5 ranged from 34.00 to 41.31 ksi while the corresponding range for 10 web tests was 39.72 to 47.26 ksi. Although the flange specimens exhibited a wide range for σ_y, the two flange specimens at a given section gave very consistent values. This indicates that material properties vary significantly along a length of steel. The standard deviation for the flange σ_y is 1.68 ksi which is 4.5% of the average σ_y = 36.98 ksi. This deviation is significant and is approximately twice that of the column sections. The large difference between the σ_y of the flange and web for the 12B16.5 (36.98 vs. 44.18 ksi) means that the actual ratio of M_p/M_y is equal to 1.28 where M_y is the moment at first yield. For equal yield stress levels in the flange and the web, M_p/M_y = 1.18. On the average yielding of the flanges would start at 0.78 M_p,

TABLE A1 SUMMARY OF TENSION TESTS

Section (1)	Statistics (2)		Statical yield stress σ_y, in ksi (3)	Ultimate stress σ_u, in ksi (4)	Elongation (8 in.), percent (5)	Strain-hardening modulus, E_{st}, in ksi (6)	Ratio of strain-hardening strain to yield strain ϵ_{st}/ϵ_y (7)
12B16.5	No. of Data		20	20	20	8	12
	Average		36.98	57.9	30.1	314	18.9
Flange	Std. Dev.		1.68	0.8	3.5	37	1.5
	Range	Min.	34.00	56.2	24.0	260	16.3
		Max.	41.31	59.1	38.5	370	22.2
	No. of Data		10	8	8	5	5
	Average		44.18	61.1	26.1	588	14.9
Web	Std. Dev.		2.37	1.0	3.0	24	0.9
	Range	Min.	39.72	59.5	23.0	480	14.3
		Max.	47.26	62.3	31.8	680	16.4
6W20	No. of Data		6	6	6	2	6
	Average		39.57	66.7	27.6	665	12.3
Flange	Std. Dev.		0.85	0.9	2.1	15	1.1
	Range	Min.	38.49	65.3	24.1	650	10.6
		Max.	40.98	67.9	30.1	680	13.8
	No. of Data		3	3	3	1	3
	Average		41.73	68.0	26.4	500	10.9
Web	Std. Dev.		0.60	1.3	1.3	-	1.8
	Range	Min.	40.99	66.3	25.3	-	8.9
		Max.	42.44	69.4	28.2	-	13.3
6W25	No. of Data		6	6	6	1	6
	Average		37.75	66.6	28.5	670	12.9
Flange	Std. Dev.		0.72	1.1	1.0	-	1.5
	Range	Min.	36.72	65.1	27.1	-	10.6
		Max.	38.92	67.4	29.9	-	15.2
	No. of Data		3	3	3	0	3
	Average		40.84	67.7	26.7	-	13.0
Web	Std. Dev.		0.70	0.6	1.6	-	2.6
	Range	Min.	39.86	67.0	24.6	-	9.4
		Max.	41.42	68.5	28.6	-	15.3

and analysis that assume elastic behavior up to 1.0 M_p could expect significant differences.

The average E_{st} in the flange of the 12B16.5 was 314 ksi, which is 0.35 of the value (900 ksi) used in the theoretical development of local buckling requirements for plastic design.[3]

The material properties for the 6W20 and 6W25 conform to the range usually encountered.

2. Cross-Section Measurements. The cross sections were measured on small lengths cut adjacent to the lengths used in the frames. Measurements were made with micrometers and vernier calipers. The average properties shown in Table A2 compare favorably with the handbook values.

The cross-section measurements were also adjacent to the lengths used for cutting the tension specimens, thus enabling M_p and the yield load P_y to be calculated. The mean values for M_p and P_y determined from the yield stresses and the corss-section measurements along with the values determined from beam tests are given in Table A3.

3. Beam Tests. Simply supported beams, loaded with two symmetrical concentrated loads to provide a uniform moment region, were tested. The purpose of these tests was to determine the plastic moment M_p and to study the lateral, local and web buckling behavior. The values of M_p determined from the beam tests are included in Table A3, and the range of data is fairly wide. The average value of M_p for the 12B16.5 was 826 kip-in. with a standard deviation of 37 kip-in.

4. Residual Stresses. The method of sectioning was used to deter-

TABLE A2 Average Section Properties

Section (1)	Number of test (2)	Flange width, b, in in (3)	Flange thickness, t, in. in. (4)	Depth d, in. in. (5)	Web thickness, w, in. in. (6)	Area A, in. ^{2} in. ^{2} (7)	Moment of inertia about x-x axis, I_x in ^{4} in ^{4} (8)	Moment of inertia about y-y axis, I_y in ^{4} in ^{4} (9)
12B16.5	24 Handbook	4.06 4.00	0.270 0.269	12.00 12.00	0.240 0.230	4.97 4.86	106.3 105.3	3.02 2.79
6W20	12 Handbook	6.11 6.02	0.368 0.367	6.32 6.20	0.269 0.258	6.01 5.90	43.8 41.7	14.0 13.3
6W25	4 Handbook	6.12 6.08	0.472 0.456	6.50 6.37	0.326 0.320	7.59 7.37	57.2 53.5	18.0 17.1

TABLE A3 Plastic Moments and Axial Yield Loads

Section (1)	Property (2)	Number of test		Average value (5)	Standard Deviation (6)	Range (7)
		Beam test (3)	Tension test (4)			
12B16.5	Plastic moment, M_p, in kip-in	2	10	826 742[a]	37	763-896
6W20	Plastic moment, M_p, in kip-in.	3	3	635 525[a]	18	601-650
	Axial yield load, P_y, in kips	-	3	243 212[a]	7	234-252
6W25	Plastic moment, M_p, in kip-in.	3	3	787 684[a]	28	744-820
	Axial yield load, P_y, in kips	-	3	292 266[a]	5	286-299

[a]Nominal value based on handbook dimensions and an assumed yield stress of 36 ksi.

mine the residual stresses and typical results are given in Fig. A1. There were no significant compressive stresses in the flanges as observed from previous studies on wide-flange sections.[2]

The usual compressive stresses at the tips of virgin flanges were removed by the continuous rotarizing process for cold-straightening the members in the rolling mill. Instead, tensile stresses are induced in the flanges, and high compressive residual stresses remain in the web. This is a more favorable distribution with regard to column strength.[2,7]

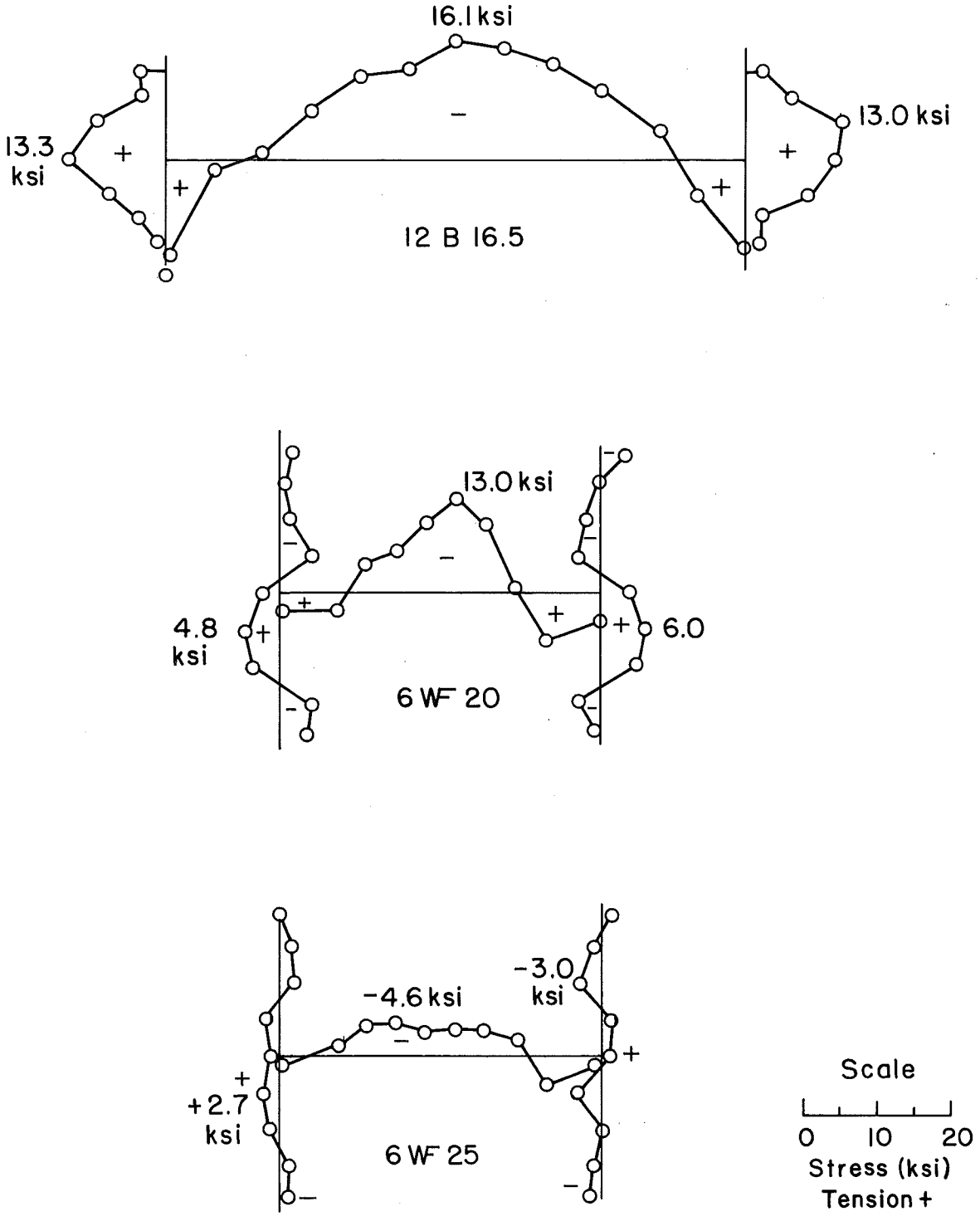

FIG. A1 TYPICAL RESIDUAL STRESS PATTERNS

9. NOTATION

The following symbols are used in this paper:

A = area of cross section;

b = flange width;

d = depth;

E = modulus of elasticity of steel (29,500 ksi);

E_{st} = strain-hardening modulus;

H = horizontal load;

I = moments of inertia, x refers to major axis, y refers to minor axis;

M_p = plastic moment capacity;

M_{pc} = plastic moment capacity considering the influence of axial load;

M_y = moment at first yield;

P = vertical load

P_y = axial yield load of cross section;

r = radius of gyration, subscripts x and y refer to major axis and minor axis, respectively;

t = flange thickness;

w = web thickness;

ϵ_{st} = strain at strain-hardening;

ϵ_y = yield strain;

σ_u = ultimate stress;

σ_y = static yield stress.

10. REFERENCES

1. Beedle, L. S.
   PLASTIC DESIGN OF STEEL FRAMES, pp. 356-377, John Wiley and Sons, Inc., New York, 1958

2. Beedle, L. S. and Tall, L.
   BASIC COLUMN STRENGTH , Proc. ASCE, 86 (ST7) pp. 139-173 (July, 1960)

3.
   COMMENTARY ON PLASTIC DESIGN IN STEEL, Manual No. 41, ASCE, 1961

4. Driscoll, G. C., Jr. et al
   PLASTIC DESIGN OF MULTI-STORY FRAMES, 1965 Summer Conference Lecture Notes, Fritz Laboratory Report 273.20, Lehigh University (1965)

5.
   FERROUS METALS SPECIFICATIONS, ASTM Standards, Part I, American Society for Testing and Materials, Philadelphia, 1964

6. Fisher, J. W.
   WELDED CONNECTIONS in "Structural Steel Design," edited by L. Tall, pp. 601-647, The Ronald Press Co., New York, 1964

7. Johnston, B. G., editor
   GUIDE TO DESIGN CRITERIA FOR METAL COMPRESSION MEMBERS, Column Research Council, pp. 11-55, 2nd ed., John Wiley and Sons, Inc., New York, 1966

8. Lay, M. G.
   THE EXPERIMENTAL BASES FOR PLASTIC DESIGN, Welding Research Council Bulletin No. 99, New York, 1964

9. Lay, M. G. and Galambos, T. V.
   THE EXPERIMENTAL BEHAVIOR OF RESTRAINED COLUMNS, Welding Research Council Bulletin No. 110, New York, 1965

10. Levi, V.
    PLASTIC DESIGN OF UNBRACED MULTI-STORY FRAMES, Ph.D. dissertation, Lehigh University, Fritz Laboratory Report 273.8 (1962)

11. Lu, L. W., Armacost, J. O. III and Driscoll, G. C., Jr.
    PLASTIC DESIGN OF MULTI-STORY FRAMES-BRACED FRAMES, Fritz Laboratory Report 273.55, Lehigh University (1968)

12. Ojalvo, M.
RESTRAINED COLUMNS, Proc. ASCE, 86 (EM5) pp. 1-11 (Oct. 1960)

13.
SPECIFICATION FOR THE DESIGN, FABRICATION AND ERECTION OF STRUCTURAL STEEL FOR BUILDINGS, American Institute of Steel Construction, New York, 1963

14. Yarimci, E., Yura, J. A. and Lu, L. W.
TECHNIQUES FOR TESTING STRUCTURES PERMITTED TO SWAY, Experimental Mechanics, 7 (8) pp. 321-331 (August 1967)

15. Yura, J. A.
THE STRENGTH OF BRACED MULTI-STORY STEEL FRAMES, Ph.D. dissertation, Lehigh University, Fritz Laboratory Report 273.28 (1965)

16. Yura, J. A.
PLASTIC DESIGN OF MULTI-STORY BUILDINGS-A PROGRESS REPORT, Engineering Journal, AISC, 2 (3) pp. 76-84 (July 1965)